AD_____
(Leave blank)

Award Number: W81XWH-08-2-0067

TITLE: Small Molecule Activators of the Trk Receptors for
       Neuroprotection

PRINCIPAL INVESTIGATOR: Nicholas J. Webster, Ph.D.

CONTRACTING ORGANIZATION: Veterans Medical Research Foundation
                          San Diego, CA 92161

REPORT DATE: May 2009

TYPE OF REPORT: Annual

PREPARED FOR: U.S. Army Medical Research and Materiel Command
               Fort Detrick, Maryland 21702-5012

DISTRIBUTION STATEMENT: (Check one)

     X   Approved for public release; distribution unlimited

     ☐   Distribution limited to U.S. Government agencies only;
         report contains proprietary information

REPORT DOCUMENTATION PAGE

Public reporting burden for this collection of information is estimated to average 1 hour per response, including the time for reviewing instructions, searching existing data sources, gathering and maintaining the data needed, and completing and reviewing this collection of information. Send comments regarding this burden estimate or any other aspect of this collection of information, including suggestions for reducing this burden to Department of Defense, Washington Headquarters Services, Directorate for Information Operations and Reports (0704-0188), 1215 Jefferson Davis Highway, Suite 1204, Arlington, VA 22202-4302. Respondents should be aware that notwithstanding any other provision of law, no person shall be subject to any penalty for failing to comply with a collection of information if it does not display a currently valid OMB control number. **PLEASE DO NOT RETURN YOUR FORM TO THE ABOVE ADDRESS.**

1. REPORT DATE (DD-MM-YYYY)	2. REPORT TYPE	3. DATES COVERED (From - To)
05/31/2009	Annual	1 May 2008 – 30 April 2009

4. TITLE AND SUBTITLE	5a. CONTRACT NUMBER
Small Molecule Activators of the Trk Receptors for Neuroprotection	W81XWH-08-2-0067
	5b. GRANT NUMBER
	5c. PROGRAM ELEMENT NUMBER

6. AUTHOR(S)	5d. PROJECT NUMBER
Nicholas Webster, Ph.D.	
Email: nwebster@ucsd.edu	5e. TASK NUMBER
	5f. WORK UNIT NUMBER

7. PERFORMING ORGANIZATION NAME(S) AND ADDRESS(ES)	8. PERFORMING ORGANIZATION REPORT NUMBER
Veterans Medical Research Foundation 3350 La Jolla Village Drive MC: 151A San Diego, CA 92161	

9. SPONSORING / MONITORING AGENCY NAME(S) AND ADDRESS(ES)	10. SPONSOR/MONITOR'S ACRONYM(S)
U.S. Army Medical Research And Material Command Fort Detrick, MD 21702-5012	
	11. SPONSOR/MONITOR'S REPORT NUMBER(S)

12. DISTRIBUTION / AVAILABILITY STATEMENT
Approved for public release; distribution unlimited

13. SUPPLEMENTARY NOTES

14. ABSTRACT

Our central hypothesis is that asterriquinone activators of the Trk receptors would prevent the neuronal cell death associated with traumatic brain injury and would improve cognitive and motor outcomes. We have developed agonists to TrkA and TrkB. The TrkA agonist has been tested in a preclinical model of cognitive impairment and a model of traumatic brain injury. The drug improves learning in a Morris water maze paradigm and reduces infarct volume in a controlled cortical impact model of brain injury. Preliminary pharmacokinetic data indicates the drug is orally available. Further analogs with improve potency and specificity are being developed.

15. SUBJECT TERMS
indole, quinone, fluorinated, nerve growth factor, brain injury

16. SECURITY CLASSIFICATION OF:			17. LIMITATION OF ABSTRACT	18. NUMBER OF PAGES	19a. NAME OF RESPONSIBLE PERSON USAMRMC
a. REPORT U	b. ABSTRACT U	c. THIS PAGE U	UU	14	19b. TELEPHONE NUMBER (include area code)

Table of Contents

Introduction

The goal of this research program is to facilitate the discovery, development and clinical evaluation of effective therapies for traumatic brain injury with emphasis on the development of lead compounds through preclinical *in-vitro* and *in-vivo* evaluation, and the conduct of pre-clinical "proof of concept" studies. Our central hypothesis is that asterriquinone activators of the Trk receptors would prevent the neuronal cell death associated with traumatic brain injury and would improve cognitive and motor outcomes. We propose to develop agonists to TrkA, TrkB and TrkC. These agonists will be tested in preclinical models of Alzheimers neurodegeneration, as an extension of our current program, and into models of traumatic brain injury with the hope of identifying lead drugs that can be taken into early trials in humans.

Body of Report

The Statement of Work in the original proposal identified the following tasks:

Task 1: *Screen combinatorial library of asterriquinone and monoquinone compounds against the BDNF receptor TrkB and the neurotrophin 3 receptor TrkC.*

We have partially completed the screen against TrkB. The library of 334 asteriquinones and 62 monoquinones were tested for their ability to activate the TrkB using an ELISA assay that detects phosphorylated TrkB. Briefly, all tyrosine-phosphorylated proteins were captured by PY20 antibody coated on microtiter plates. The presence of TrkB among the phosphorylated proteins was then detected by anti-TrkB antibodies. Activation of TrkB was compared to stimulation by a maximal concentration of BDNF (100 ng/ml). In this assay, the original compound DAQ-B1 did not activate TrkB and our lead drug 5E5 activated to 74% the effect of BDNF. This is a little higher than the activation we measured by immunoblotting whole cell extracts (~40%) but may simply reflect the difference between the ELISA and western blot (1). Thirty-nine compounds had activity >25% BDNF. These compounds are being verified in secondary activation assays.

Task 2: *Model structure activity relationships for TrkB or TrkC activation using forward feed neural networks and multiple linear and nonlinear regression. Screen library of theoretical structures in silico using the derived models.*

We have modeled the activity of our compounds against TrkA, the insulin receptor, and for toxicity. The data for activity against the insulin receptor were generated under earlier funding from the American Diabetes Association but are included here in the modeling as a control for specificity. While not proposed in the original grant application, we felt that eliminating compounds that are insulin mimetics would help prevent any hypoglycemic complications. The top 30 predictions with good TrkA activity are:

Substitent 1	Substituent 2	Substituent 3	Substituent 4	Substituent 5	Substituent 6	Substituent 7	Predicted Trk activation	Predicted IR activation	Predicted survival at 3 uM	Predicted survival at 10 uM
HYDROGEN	HYDROGEN	HYDROGEN	HYDROGEN	HYDROXYL	METHOXYL	HYDROGEN	0.677466	0.885382	0.840618	0.760427
HYDROGEN	HYDROGEN	HYDROXYL	HYDROGEN	FLUORO	HYDROGEN	HYDROGEN	0.67652	-0.0287032	0.840619	0.726363
HYDROGEN	HYDROGEN	HYDROGEN	FLUORO	FLUORO	HYDROGEN	HYDROGEN	0.675634	0.172545	0.841529	0.80324
HYDROGEN	HYDROGEN	HYDROGEN	HYDROGEN	HYDROXYL	HYDROGEN	FLUORO	0.674982	1.015	1.054	0.757823
HYDROGEN	HYDROGEN	HYDROGEN	HYDROGEN	FLUORO	METHYL	HYDROGEN	0.674344	0.928875	0.841196	0.783958
HYDROGEN	HYDROGEN	HYDROGEN	HYDROGEN	FLUORO	PHENYL	HYDROGEN	0.674344	0.928875	0.841196	0.783958
HYDROGEN	METHYL	HYDROGEN	HYDROGEN	HYDROXYL	HYDROGEN	HYDROGEN	0.673807	1.01496	0.840618	0.729168

|										
PROPYL	HYDROGEN	HYDROGEN	HYDROGEN	HYDROXYL	HYDROGEN	HYDROGEN	0.672285	-0.0406381	0.840618	0.727924
ISOPROPYL	HYDROGEN	HYDROGEN	HYDROGEN	HYDROXYL	HYDROGEN	HYDROGEN	0.670009	-0.0406381	0.840618	0.728284
HYDROGEN	HYDROGEN	METHOXYL	HYDROGEN	FLUORO	HYDROGEN	HYDROGEN	0.669731	-0.0392314	0.840633	0.728592
METHYL	HYDROGEN	HYDROGEN	HYDROGEN	HYDROXYL	HYDROGEN	HYDROGEN	0.669715	-0.0406381	0.840618	0.729242
HYDROGEN	HYDROGEN	HYDROGEN	HYDROGEN	BROMO	PROPYL	HYDROGEN	0.66825	0.0332232	1.054	1.0648
HYDROGEN	HYDROGEN	HYDROGEN	HYDROGEN	FLUORO	HYDROGEN	HYDROXYL	0.668072	1.015	1.054	0.919918
HYDROGEN	HYDROGEN	HYDROGEN	HYDROGEN	CHLORO	PROPYL	HYDROGEN	0.666432	0.0713229	1.054	1.02929
HYDROGEN	HYDROGEN	HYDROGEN	HYDROGEN	CYCLOPROPYL	BENZYL	HYDROGEN	0.666432	0.0713229	1.054	1.02929
HYDROGEN	HYDROGEN	HYDROGEN	HYDROGEN	CYCLOPROPYL	BROMO	HYDROGEN	0.666432	0.0713229	1.054	1.02929
HYDROGEN	HYDROGEN	HYDROGEN	HYDROGEN	CYCLOPROPYL	CHLORO	HYDROGEN	0.666432	0.0713229	1.054	1.02929
HYDROGEN	HYDROGEN	HYDROGEN	HYDROGEN	CYCLOPROPYL	CYCLOPROPYL	HYDROGEN	0.666432	0.0713229	1.054	1.02929
HYDROGEN	HYDROGEN	HYDROGEN	HYDROGEN	CYCLOPROPYL	FLUORO	HYDROGEN	0.666432	0.0713229	1.054	1.02929
HYDROGEN	HYDROGEN	HYDROGEN	HYDROGEN	CYCLOPROPYL	HYDROXYL	HYDROGEN	0.666432	0.0713229	1.054	1.02929
HYDROGEN	HYDROGEN	HYDROGEN	HYDROGEN	CYCLOPROPYL	IODO	HYDROGEN	0.666432	0.0713229	1.054	1.02929
HYDROGEN	HYDROGEN	HYDROGEN	HYDROGEN	CYCLOPROPYL	ISOPROPYL	HYDROGEN	0.666432	0.0713229	1.054	1.02929
HYDROGEN	HYDROGEN	HYDROGEN	HYDROGEN	CYCLOPROPYL	METHOXYL	HYDROGEN	0.666432	0.0713229	1.054	1.02929
HYDROGEN	HYDROGEN	HYDROGEN	HYDROGEN	CYCLOPROPYL	METHYL	HYDROGEN	0.666432	0.0713229	1.054	1.02929
HYDROGEN	HYDROGEN	HYDROGEN	HYDROGEN	CYCLOPROPYL	PHENYL	HYDROGEN	0.666432	0.0713229	1.054	1.02929
HYDROGEN	HYDROGEN	HYDROGEN	HYDROGEN	CYCLOPROPYL	PROPYL	HYDROGEN	0.666432	0.0713229	1.054	1.02929
HYDROGEN	HYDROGEN	HYDROGEN	HYDROGEN	BROMO	ISOPROPYL	HYDROGEN	0.665809	0.0150583	1.054	1.07253
HYDROGEN	HYDROGEN	HYDROGEN	HYDROXYL	FLUORO	HYDROGEN	HYDROGEN	0.664877	0.0638881	0.842474	0.847652
HYDROGEN	HYDROGEN	HYDROGEN	HYDROGEN	IODO	PROPYL	HYDROGEN	0.663659	-0.0023704	1.054	1.08285
HYDROGEN	HYDROGEN	HYDROGEN	HYDROGEN	CHLORO	ISOPROPYL	HYDROGEN	0.663402	0.0398269	1.054	1.04808

These structures have been given to Prof. Pirrungs group for synthesis. Mathematical modeling of the TrkB and TrkC agonists is waiting for the completion of the in vitro screens.

Task 3: *Synthesize new asterriquinone and monoquinone compound libraries based on the mathematical modeling predictions.*

This project period was focused on two main goals: the preparation of quantities of our lead compound, 5E5, sufficient to support animal studies; the preparation of fluorinated indoles and their conversion to 5E5 analogues. The scope of the work was a quite substantial amount of the 5E5 drug substance, in pure and crystalline form, and a half-dozen 5E5 analogues.

The synthesis of 5E5 is performed using a method earlier developed in our lab (2). It entails the acid-promoted condensation of 7-fluoroindole (**1**) with dichlorobenzoquinone, an *in situ* oxidation to give **2**, and then a solvolysis. Two methods have been used for the last step. The most direct is methanolysis, with hydroxide in methanol (Scheme 1). Sometimes, however, this reaction gives the dihydroxyquinone, which must then be methylated with dimethyl sulfate. Early work used
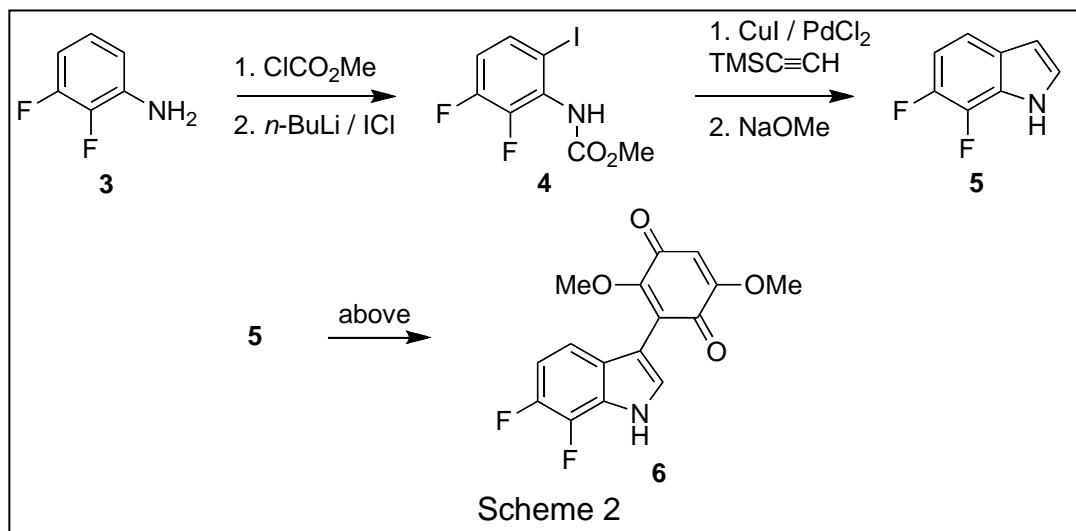

Scheme 1
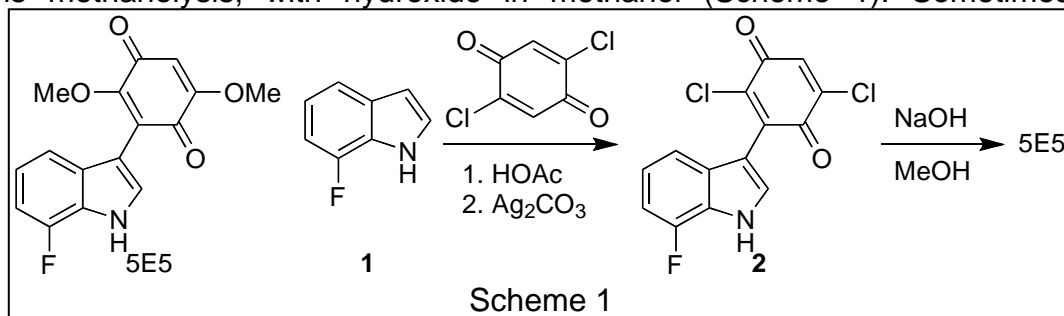
the latter procedure to prepare about 1 g of 5E5. Later work was able to perform this

5

conversion in a single step. We used this method to prepare our most recent sample of ca. 400 mg of 5E5. After chromatography, pure 5E5 was obtained that is a crystalline solid. Its recrystallization gives a highly pure sample of material that is very desirable for *in vivo* studies.

Other indoles have been prepared for conversion to 5E5 analogues by one of two routes. Shown in Scheme 2 is the method applied to fluorinated anilines, which are commercially available. The amine is protected, which activates the adjacent CH bond for metalation and iodination. The resulting compound **4** is then coupled with a monoprotected acetylene using the Sonogashira reaction. Treatment with base removes its protecting group, causes closure of the heterocyclic ring, and deprotects the nitrogen, all in one step. The desired 6,7-difluoroindole (**5**) is the result.

Scheme 2

That compound could be subjected to the same route used to prepare 5E5 to access **6**.

Indoles **7**-**9** are also in hand (Scheme 3); the Sonogashira route was also used to prepare them from the corresponding anilines. For the remaining targeted indoles **10** and **11**, a different route was used. The Bartoli reaction is an excellent method to prepare indoles from nitrobenzenes (3), which are broadly available with a wide variety of substitution patterns. For example, the nitrobenzene precursors to **10** and **11** are available commercially or in a single step from a

Scheme 3
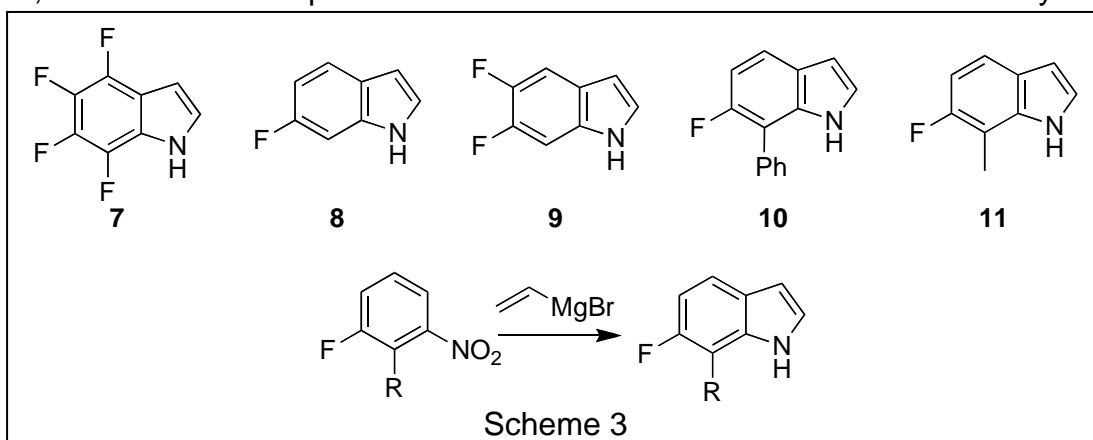
commercial material. Their Bartoli reactions are excellent processes to generate **10** and **11**.

Task 4: *Retest new compounds against TrkB and TrkC and for toxicity and refine mathematical models. Rerun in-silico predictions using theoretical library.*

Task 4 is awaiting the synthesis of the new indole quinones by Prof Pirrung's group.

Task 5: _Synthesize selected asterriquinone and monoquinone structures based on second round of predictions._

Task 5 is awaiting the synthesis of the new indole quinones by Prof Pirrung's group.

Task 6: _Test selected compounds for potency and selectivity for activation of Trk receptors. Test ability of compounds to support neuronal differentiation and neuronal survival using neuronal cells in culture._

Task 6 is awaiting the synthesis of the new indole quinones by Prof Pirrung's group.

Task 7: _Test selected compounds for neuroprotective effects in a mouse model of neurodegeneration._

The original proposal proposed testing our compunds in the PDAPP model for Alzheimers disease. These studies are ongoing as the PDAPP model was delayed due to breeding problems with these animals. We started with two breeding pairs from Jackson Labs. While these animals were able to breed, the litters were continually eaten by the parents. After looking various variables, it appeared that the mice were very sensitive to post-natal disturbances and would respond by eating the litters. We found that the regular mouse husbandry provided by the vivarium staff was causing enough of a disturbance that we failed to keep litters. Once we had discovered this problem, we worked with the staff to minimize the handling of cages and mice and were able to reverse the trend. This investigative phase, however, delayed the generation of the PDAPP mice for testing. We now have 100 PDAPP transgeinc mice of various ages. Some are being tested in a prevention trial with 5E5 starting at 6 months of age as originally proposed, whereas others are being allowed to age to 10-12 months for a reversal study.
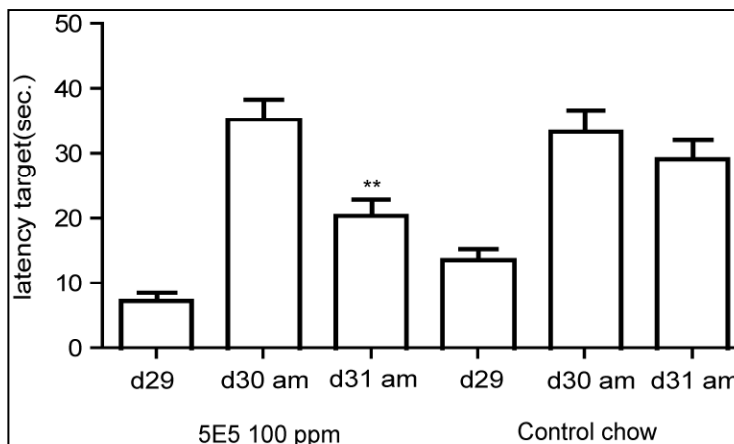

Figure 2. Ability of mice to learn the new position of the hidden platform in a Morris water maze. Mice were fed normal chow or the same diet supplemented with 100 ppm 5E5. Graph shows the latency to find the hidden platform (day 29), which measures retention of a previously learned position, and to learn the new position of the hidden platform (days 30 & 31). Mice are trained on the new location on days 30 and 31. Data were analyzed by ANOVA with Tukey post-hoc analysis.

As the PDAPP mice were delayed, we decided to test our lead compound 5E5 in a reversal study in NGF+/- mice. We had previously shown that 5E5 preventyed the onset of cognitiver decline but wew wanted to test whether 5E5 would reverse pre-existing impairments. Mice were 10-11 months, an age after cognitive impairment has occured. We used a higher dose of 5E5 in the diet in the reversal study as we felt that this was a more stringent test of our compound. The study design was the same as the earlier prevention study except the animals were 11-12 months and the drug was included at 100 ppm in the diet. All mice learned the platform during the initial acquisition phase and then were randomized into drug-treated or control chow groups. After one
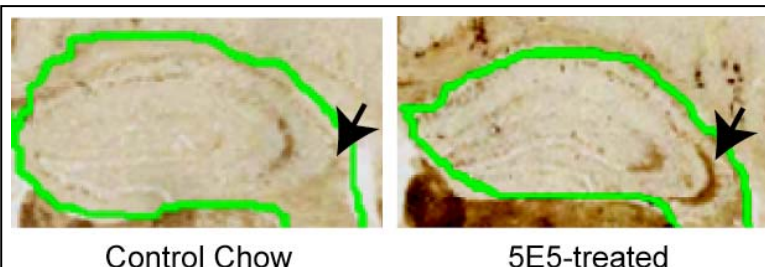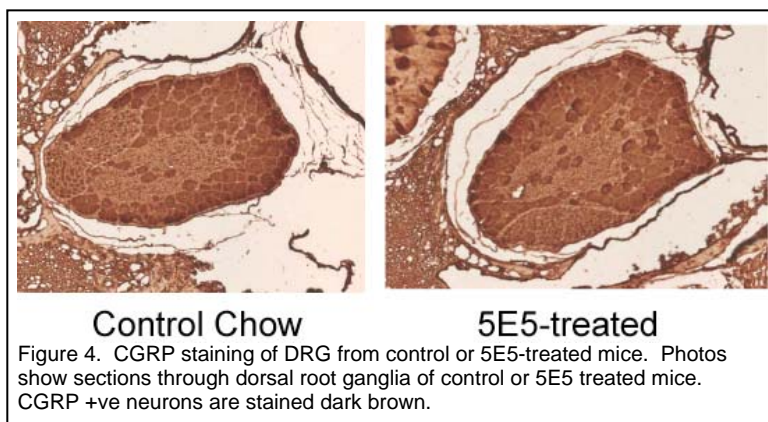

Figure 3. Hippocampal ACHE staining. Arrow points to CA3 region. Green outlines hippocampus. ACHE staining is brown.

month on drug, the mice were tested then retrained on a hidden platform in the second location. All mice membered the first platform position when tested on day 29 but the drug treated mice appeared to find it faster but the difference did not quite make significance (Fig. 2). The drug-treated mice decreased time taken to reach the platform on the second day of training but the control group did not. The mice on the control chow took the same amount of time to find the platform on the second day (day 31) as the first (day 30) showing their inability to learn the platform location.

Figure 4. CGRP staining of DRG from control or 5E5-treated mice. Photos show sections through dorsal root ganglia of control or 5E5 treated mice. CGRP +ve neurons are stained dark brown.

The drug increased ACHE staining in the CA3 region of the hippocampus consistent with increased cholinergic neuron content (Fig. 3). The mice swam identical distances during the probe test in both studies so the drug did not alter motor activity, and liver enzymes were not altered in either study, although we observed a little reversible steatosis on the 100 ppm diet. The drug did not cause sprouting of DRG peripheral sensory neurons in these mice. Peripheral neurons are labeled for CGRP (Fig. 4). Dark brown indicates cell bodies of CGRP+ve neurons. No sprouting is evident. Overall, our data indicate that treatment with the drug 5E5 improves the ability of NGF+/- mice to learn spatial information after the onset of cognitive impairments.

Task 8: _Test selected compounds for neuroprotective effects in a mouse controlled cortical impact (CCI) model of traumatic brain injury._

The CCI model was used as described elsewhere (4). The CCI tests aimed to measure the dimension of neuronal cell death in the brain lesion after CCI was elicited at 5 m/sec velocity, depth 1.2 mm. This experimentation was used for initial _in vivo_ testing of the 5E5 drug effects on overall dimension of brain trauma after 14 days of preconditioning with compound submitted to animals as an admixture in normal chow at ~100 ppm (~20 mpk). The control and treated animals were sacrificed at 6h, 24h and 48h following the cortical impact. The whole head paraffin histology method was applied to assess neuropathological parameters. Lesion volume morphometry was performed using virtual image analysis and ScanScope software (Aperio Tech. Inc.) on the histological specimens prepared for treated and untreated animal groups at a time course of 6, 24, and 48 hrs. The identity of the individual animal was blinded to the investigator. The data for these two experimental groups were obtained in a cohort of 6-8 animals per time point:

The aim of this pilot study was to obtain quantitative characteristics of brain tissue damage such as 1) the size (area) of brain lesion that can be used to perform volume calculation, 2) the percentage of hemorrhagia, and 3) the dimension of acute/chronic neuronal cell death using Masson's trichrome stain (American Master*Tech Scientific, Inc. Lodi, CA, US). After manual annotation of the impact foci, image analysis tools were tuned and employed to perform morphometry of this histochemical staining. To calculate brain lesion volume, the brains were cut into five equally spaced 2 mm coronal slabs with three cross sections placed on the rostral and caudal edges and in the middle of the cortical lesion. The H&E and Masson's trichrome stained sections were digitalized using Aperio scanning system. Using the pen tool, virtual slides were annotated by encircling the lesion edges (penumbra)
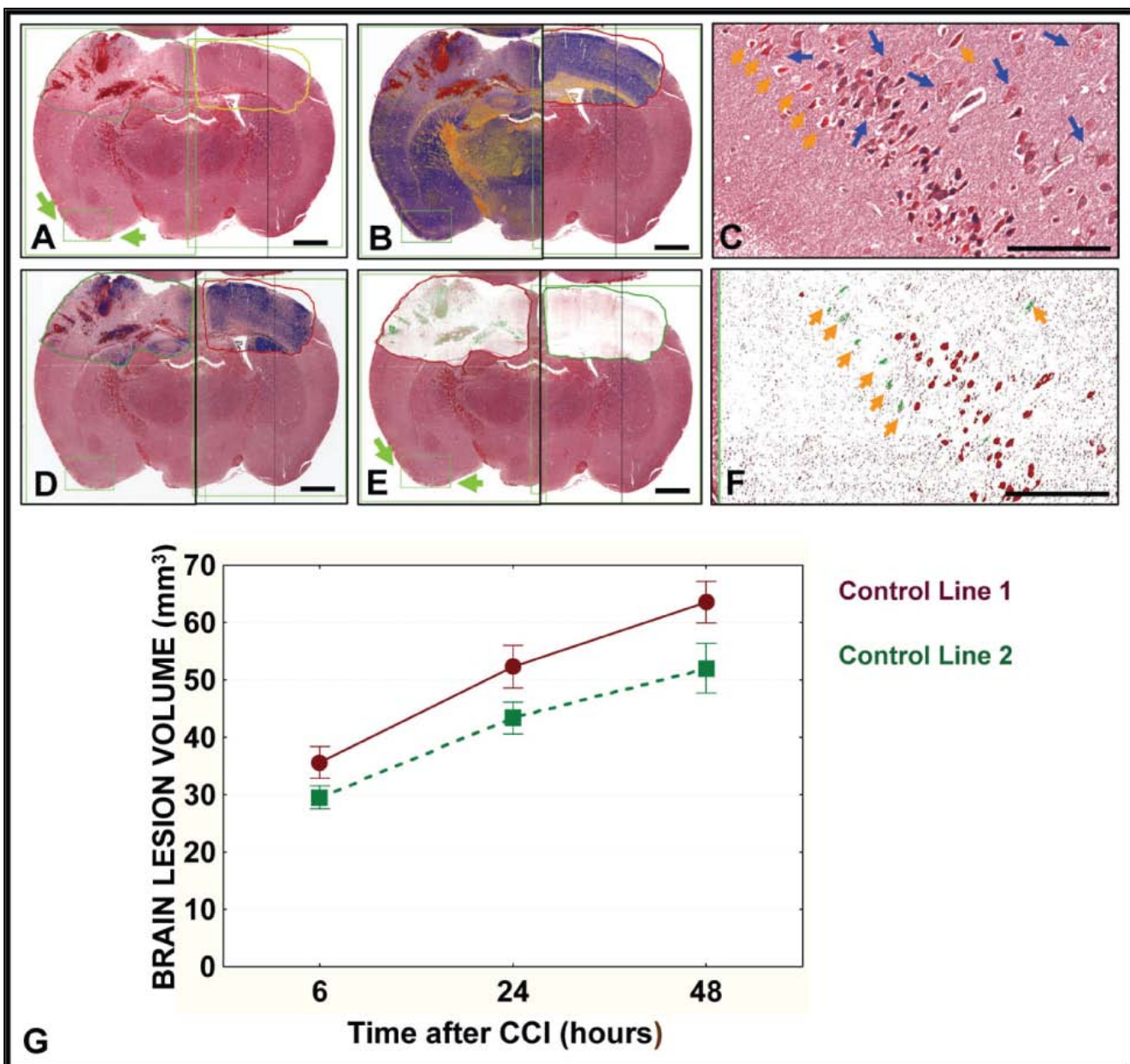
Figure 5: Algorithm-assisted analysis of brain lesions. Tissue sections from mice subjected to CCI were stained with Masson's trichrome stain. The digital slide image (A) presents the core lesion in the left hemisphere and intact contralateral right hemisphere with selected regions of interest. Application of color deconvolution (B), nuclear (D), and color colocalization (E) algorithms resulted in generation of mark-up images. (B) Micro-hemorrhage areas are indicated by red color, early ischemic changes in the gray matter by yellow, normal brain tissue by blue. (C) Necrotic (bright red; yellow arrows), apoptotic (pyknotic; dark blue) and normal (blue arrows) neurons in the *contrecoup* focus in the digital slide image (E; green arrows) are visualized as green (necrotic) or red (apoptotic) cells in the corresponding mark-up image (F). Bars on macroimages correspond to 1 mm, on high-zoom images to app. 100 µm. Graphical presentation of average volumes of brain lesions in control lines 1 (brown) and 2 (green). Markers depict mean volume, whiskers SEM. P values for 6 h, 24 h, and 48 h time points equal 0.1, 0.07, and 0.06, respectively.

between intact and pathologically changed brain tissue, and the lesion area (mm2) was reported in annotation window. The rostral-caudal dimensions of the foci were determined through the use of a stereotaxic atlas for the mouse brain, which was viewed electronically side by side with the coronal section images. Distance (mm) between coronal coordinates for bregma +1.54 (rostral position) and -3.88 (caudal position) determined distribution of the lesion volume and was multiplied by the sum of lesion areas (mm2) from all cross sections, yielding the total lesion volume (mm3). The proposed calculation is based on Cavalieri's method that was modified by us for the purpose of volumetric analysis performed on digital slides. Figure 5 demonstrates this method, which was recently published in J Histochem Cytochem (5).

This preliminary analysis revealed smaller contusion area and volume following drug pretreatment, suggesting protective effect.

9

Since PI lab is fortunate to have Aperio CS-1 slide scanning system with associated ScansScope software package which includes algorithms for image analysis (Apereio Technology Inc., Vista, CA), we focused our efforts on the following goals: 1. Training and tuning of simple and combinatorial algorithms to make them reliable in the global and fine morphometric evaluation of post-traumatic changes in the brain and 2. In particular, our goal was to assess the amount of neurons with early and late stages of apoptotic and/or necrotic changes, and in addition the extent of posttraumatic bleedings and micro-heamorrhagic foci.

To proceed with these goals, PI laboratory successfully launched the 5E5 Project image database on BIMR server based on Aperio Scanscope System with incorporated internet platform enabling scanning, archiving or investigating entire slides with assisted software over the internet. This digital pathology tool and system was used to create project group folders with password protected access over the internet to all virtual slide images including H&E and Masson-Trichrome stainings of all cases. In ongoing PI collaboration with Dr. Olson (Aperio Technology Inc.), who developed and provided us with new generations of multicolor deconvolution and combinatorial algorithms, particularly the novel colocalization algorithm, we succeeded in tuning of algorithm panel which will allow us to conduct the study according to the proposed aim. As provided working example in **Figure 6 and Table 2**, training and tuning simple and combinatorial algorithms made them useful and reliable in unbiased global and fine morphometric evaluation of the traumatic changes in the brain. The measurement principles with mark-up examples of variety of algorithms are presented on the panels below, where we compared injured ipsi- and healthy contralateral hemispheres. Initially we tested and modified thresholding of the image segmentation in our basic algorithms measuring positive pixel values after color deconvolution in cytoplasm or nuclear compartments **(SP10; SP3, SP13)**. Lately, we worked with the sophisticated algorithms covering multiple spectra of colors resulting in generation of signals indicating colocalization of two or more colorimetric signals in the same brain area or cell compartments **(SP34, SP34LL, SP8).** The whole hemisphere measurements were contrasted with free hand tool annotation of selected areas encompassing infarct or intact brain. As indicated in **Table,** the trained and adjusted algorithms have a power to measure the areas occupied by micro-hemorrhages and/or odema **(SP10, SP3, SP34, SP34LL),** global number and percentage of dying neurons in the affected areas in comparison to the control hemisphere **(SP3, SP8, SP13).** We believe that the set of algorithms and macros which we have already prepared will be sufficient for the correlative histological and immunohistochemical investigations to characterize the cellular response in our treated and untreated with 5E5 experimental groups.

Table 2: Algorithms: *D*econvolution, *C*olocalization, *N*uclear and *I*ntensity/Pizels

	Area (mm^2)	%Haemorrhage&Edema	% Intact Grey Matter	% Apoptotic/Necrotic
SP10 Infarct (D)	4.027	**20.79** (red; haem)	42.082 (blue)	NR
SP10/ctrl hem (D)	3.763	1,472 (red)	59.342 (blue)	Neurons appr. 1%
SP3 Infarct (D)	8.175	**23.58** (red; haem)	51.596 (orange)	Neurons %?
SP3/ctrl hem (D)	5.655	17.655 (red; WM; edema)	71.606	Neurons %?
SP13 Infarct (I+N)	8.963	14.399 (red/orange;nuclei)	85.6 (blue; nuclei)	Neurons %?
SP13/ctrl hem (I+N)	6.487	6.29 (red/orange;nuclei)	93.709 (blue; nuclei)	Neurons appr. 1%
SP34/Infarct (C)	7.935	**28.42** (Cyan)	42.26 (magenta)	NR
SP34/ctrl hem (C)	5.589	18.00 (Cyan; odema)	58.9 (magenta)	NR
SP34LL/Infarct (C)	8.963	**26.57** (Cyan; odema)	55.753 (green)	**18.739** (black)

SP34LL/ctrl hem (C)	6.503	19.936 (Cyan; WM; edema)	51.456 (green)	**7.726** (black)
SP8/Infarct (C-old)	9.036	**29.093** (green; haem)	NR	NR
SP8/ctrl hem (C-old)	6.503	**1.379** (green; haem)	NR	NR

CRE3-WT 6 hr after CCI; Trained Algorithms Examples
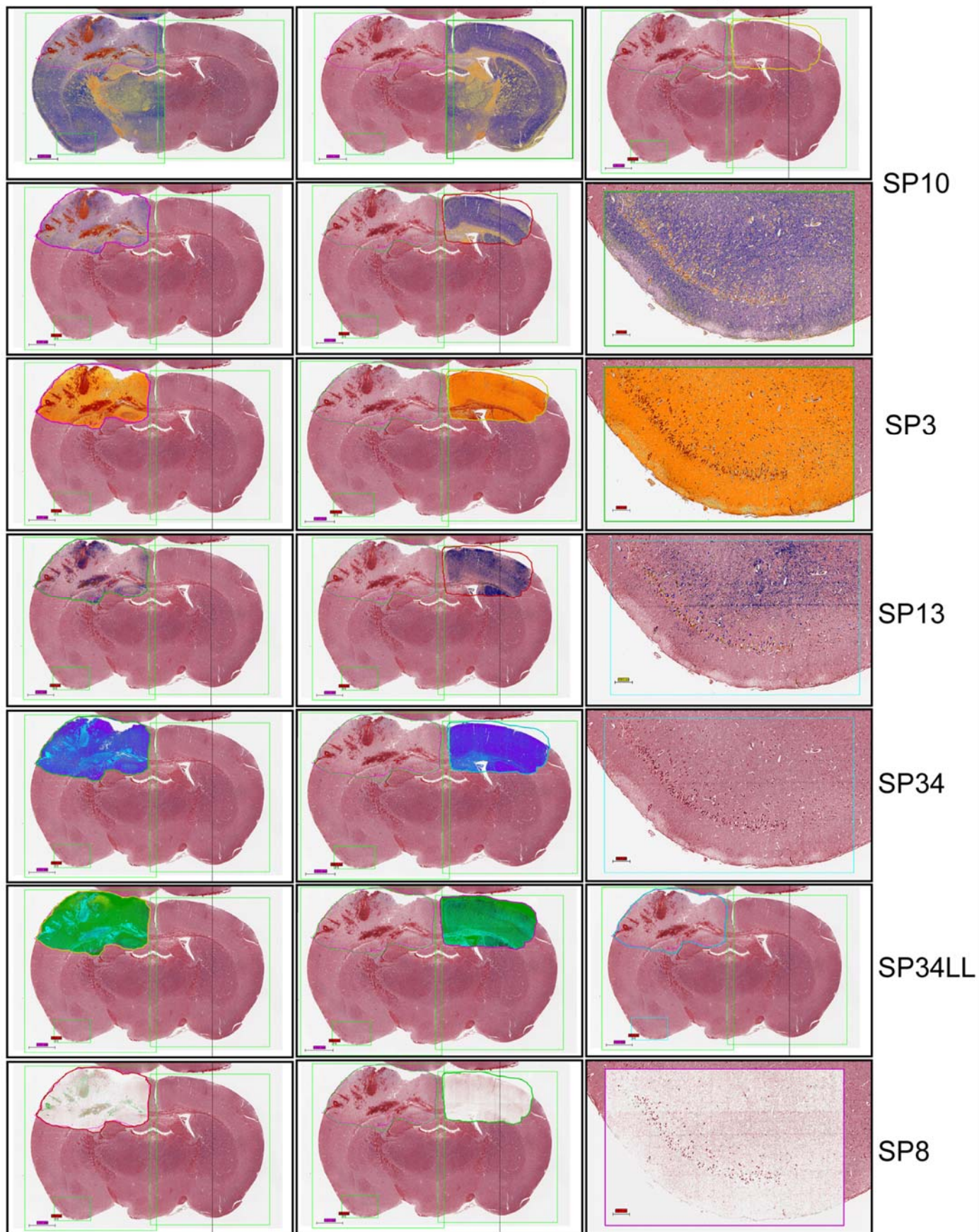

SP10

SP3

SP13

SP34

SP34LL

SP8

Figure 6: Demonstration of the performance of the algorithms used to measure infarct volumes. Labeling is given in main report text.

**Task 9:** Determine pharmacokinetic properties of compounds in mice.

An aim of our proposal was to obtain preliminary pharmacokinetic data for our drug 5E5 in rodents. We contracted with a PK core at the Burnham Institute to perform a PK analysis in mice. 5E5 was administered at 0.2 mpk by oral gavage. Plasma concentrations were measured by LC/MSMS by the Pharmacology Core at the Burnham Institute. Plasma 5E5 was maximal by 30-60 min (Fig. 7). By 4 h the concentration had fallen to 25% max. The AUC_{0-6} was 4434 ng*hr/mL. The predicted logP value for 5E5 is -0.7 and the compound obeys Lipinski's rules, so the compound should have good bio-availability. The finding of improved learning in the 5E5 treated animals also suggests that the drug must enter the brain.

The animal studies required the preparation of a chow by the evaporation of an ethanol solution of 5E5 mixed into the mouse chow. We observed during the PK study that 5E5 itself is metabolized following oral administration and a second stable metabolite is observed by LC. The PK core had difficulty establishing an LC/MSMS assay for 5E5 as it is not stable under the MSMS conditions. Only a very small parent ion peak is observed with pure

Figure 7 Plasma concentrations of 5E5 following oral dosing.

5E5 in DMSO but a major peak M^+-28 is observed, which we believe is loss of CO from the molecule under the ionization conditions.   It may prove to be the case that 5E5 is a pro-drug form and the actual active agent for neuroprotection is the monohydroxy or even the dihydroxy compound. It is important for us to establish the identity of this species as it may be the true drug that has neuroprotective effects.
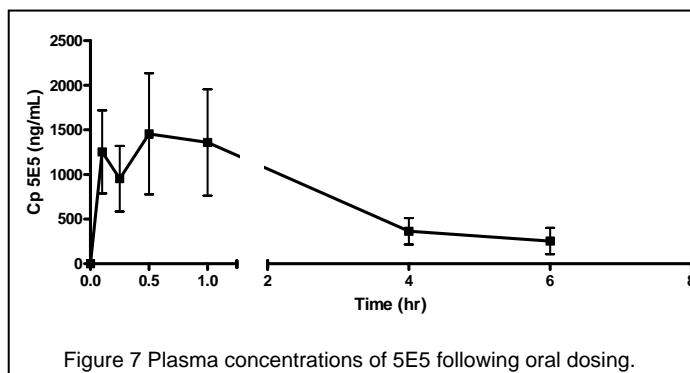
Key Research Accomplishments

- Substitution on the 1 and 5 positions are predicted to give good TrkA activation with low IR activation and good survival
- Acid-catalyzed condensation of indoles with dichlorobenzoquinone is a facile method to make mono-indolyldihydroxybenzoquinones
- The Sonogashira reaction with monoprotected acetylenes can be used to create substituted indoles
- Lead drug 5E5 reverses cognitive decline in the NGF+/- mouse model
- Lead drug 5E5 increases cholinergic neuron staining in CA3 region of hippocampus
- Lead drug 5E5 does not cause peripheral neuron sprouting
- Lead drug 5E5 has good pharmacokinetic profile in mice
- Lead drug 5E5 reduces infarct volume in Controlled Cortical Impact model of TBI.
- Automated slide processing with Digital Pathology Tools allows rapid unbiased assessment of brain injury

Reportable Outcomes

None

Conclusion

The methods developed in this project give us the tools to prepare a large and diverse family of candidate neuroprotective agents. Because these compounds are all small molecules with a

relatively modest polar surface area, they should have no difficulty penetrating to the brain, a significant issue with most other drugs (especially neurotrophins) aimed at treating brain injury. Indeed the pharmacokinetic data indicate that the drug is readily absorbed and dispersed following oral administration. The pre-clinical in vivo testing of 5E5 compound showed promising results reducing infarct volume in the controlled coritical impact model of brain injury and in restoring cognitive function in a neurotrophin-deficient model of impaired learning suggesting that it could have potential utility in the treatment of acute traumatic and neurodegenerative diseases. These compounds could lead to a therapeutic for TBI that is easy and economical to manufacture and simple to administer.

References

1. Bo Lin, Michael C. Pirrung, Liu Deng, Zhitao Li, Yufa Liu and Nicholas J.G. Webster. (2007) Neuroprotection by small molecule activators of the NGF receptor. J. Pharmacol. Exp. Ther. 322:59-69. PMID17468299
2. Pirrung, M. C.; Park, K.; Li, Z. Synthesis of 3-indolyl-2,5-dihydroxybenzoquinones. *Org. Lett.* 2001, *2*, 365. Pirrung, M. C.; Deng, L.; Li, Z.; Park, K. Synthesis of 2,5-dihydroxy-3-(indol-3-yl)-benzoquinones by acid-catalyzed condensation. *J. Org. Chem.* 2002, *67*, 8374.
3. Pirrung, M. C.; Wedel, M.; Zhao, Y. 7-Alkyl indole synthesis via a convenient formation/alkylation of lithionitrobenzenes and an improved Bartoli reaction. *Synlett* 2002, 143.
4. Bermpohl D, You Z, Korsmeyer SJ, Moskowitz MA, Whalen MJ (2006) Traumatic brain injury in mice deficient in Bid: effects on histopathology and functional outcome. J Cereb Blood Flow Metab 26:625-633.
5. Krajewska M, Smith LH, Rong J, Huang X, Hyer ML, Zeps N, Iacopetta B, Linke SP, Olson AH, Reed JC, Krajewski S (2009). Image Analysis Algorithms for Immunohistochemical Assessment of Cell Death Events and Fibrosis in Tissue Sections. J Histochem Cytochem 2009 Mar 16. [Epub ahead of print]

Appendices

None